© Universiti Tun Hussein Onn Malaysia Publisher's Office

IJIE

http://penerbit.uthm.edu.my/ojs/index.php/ijie
ISSN : 2229-838X e-ISSN : 2600-7916

The International Journal of Integrated Engineering

Mapping of Potential Groundwater Using Electrical Resistivity Imaging (ERI) at Low Land Area of Parit Raja Johor

Akhtar Izzaty Riwayat[1,3], Mohd Ariff Ahmad Nazri[1,2*], Noor Aliza Ahmad[1]

[1]Faculty of Civil Engineering and Built Environment,
Universiti Tun Hussein Onn Malaysia, 86400 Parit Raja, Johor, MALAYSIA

[2]Eco Hydro Technology Research Centre
Universiti Tun Hussein Onn Malaysia, 86400 Parit Raja, Johor, MALAYSIA

[3]Research Centre for Soft Soil (RECESS),
Universiti Tun Hussein Onn Malaysia, 86400 Parit Raja, Johor, MALAYSIA

*Corresponding Author: ariffn@uthm.edu.my

DOI: https://doi.org/10.30880/ijie.2022.14.09.003
Received 25 April 2022; Accepted 15 July 2022; Available online 30 November 2022

Abstract: Electrical Resistivity Imaging (ERI) has emerged as an important technique in geophysical surveys for gaining more information and locating hidden water. This method was used at Parit Raja, Johor to investigate the location of underground water storage. Two-dimensional (2D) geoelectrical imaging has been used for this study. The imaging method was used at three different locations in the study area to identify potential aquifer and suitable locations for boreholes that would serve as observation wells. A Schlumberger array was set up during data acquisition since it can imagine deeper profile data and suitable for areas with a homogeneous layer. For 2D subsurface images, the raw data were processed with the RES2DINV software. According to the ERI results, this area was dominant with low resistivity values of less than 10 Ωm and potential shallow aquifer depths ranging from 10 to 30 m. Furthermore, the chargeability value obtained from Induced Polarization (IP) supported this point. According to the IP data, the chargeability at that point was between 0 and 1 ms, indicating the presence of a groundwater in the study area.

Keywords: Electrical resistivity imaging (ERI), groundwater, Schlumberger array, Parit Raja

1. Introduction

Geophysical methods are techniques commonly used by geophysicists to discover the earth surface by using physics principles. In many studies, geophysics has grown to investigate subsurface, such as groundwater, minerals, and hydrocarbons. This method used to interpret soil properties, layers, and the composition of the subsoil, cavities, structures, or bodies of water commonly found in soils with different physical properties than their geological environment [1]. Due to time, cost, and quality concerns, geophysical methods are known for their effectiveness in civil engineering compared to most conventional methods [2]. It was crucial in the preliminary surveys, particularly in determining the surface condition. Geophysical methods are superior to traditional methods for groundwater exploration, which improves understanding of groundwater sources as water becomes more valuable and scarcer. Well drilling is a conventional method for directly exploring underground water systems; however, the cost of drilling a well is prohibitively expensive. Furthermore, a sufficient number of tubes well are required to interpret the depth and area of various geological formations,

Electrical Resistivity Imaging (ERI) is the most commonly used in the geophysical method. ERI studies aim to determine resistivity distribution beneath the surface by measuring the soil surface [3]. Furthermore, ERI aids in the visualization of the geological environment to indicate the presence of aquifer layers. For decades, it has been used to determine the thickness and resistivity of layered media. This non-destructive method minimizes site disruption and damage of soil surface [4]. ERI is considered a sustainable technique due to preserving the environment during data acquisition. This technique also resolves a few of the issues encountered by most conventional land survey techniques [4]. In addition, this method is well-known for its low cost and cost-effectiveness. However, under continuous conditions, it can provide dependable physical characteristics [5]. Conventional methods are inefficient since the method only provides information on actual drilling points, requiring interpolation between boring determinations to determine conditions that may be uncertain [6]. Conventional methods are currently used as a reference and to compare the ERI results to interpret a general overview of the study area.

Since groundwater movement is primarily localized and difficult to determine, ERI has proven the most effective technique for mapping groundwater sources [7]. Reliable groundwater information can be obtained with the help of supporting borehole data and interpretations of acquired resistivity imaging. In Malaysia, ERI has been used to solve various problems, particularly in civil engineering and research. Subsurface failure and underground contamination are two of the most common issues encountered in the field. The successful implementation of these tools has assisted engineers in identifying subsurface failure sources, thereby preventing damage to surrounding structures and materials [6]. The groundwater sources are defined by geological factors based on structure, geological sequence, and stratigraphic distribution of hydrological units. The recharge rate is also an essential factor in determining groundwater availability in the area. Groundwater recharge occurs in the aquifer via the following mechanisms: direct rain infiltration, river infiltration, and lateral subsurface inflows through fractures. Groundwater is being assessed and explored using various geophysical techniques since the close relationship between aquifer electrical and hydrogeological properties [8]. Therefore, this study aims to interpret the potential location of groundwater in the low land area located in Parit Raja, Johor.

2. Material and Method

2.1 Study Area

Universiti Tun Hussein Onn Malaysia (UTHM) campus is located in south peninsular Malaysia northeast from capital of Johor Bahru with an area of about 54.32 acre and coordinates of 1.8586°N and 103.0856°E within Parit Raja, Batu Pahat Johor. The topography area is generally flat and low-lying, with local elevations at the site ranging around 0.5 m to 2.0 m above the mean sea level [9]. The region has a humid tropical climate with average rainfall ranging between 2250 to 2600 mm/year and temperatures between 24°C and 33°C. UTHM is located 20 km from the coastal area of Pantai Rengit and has layers of sediments and fossils formed due to tidal effects that indirectly affect undesirable concentrations [10]. Similar to a study by [11], the UTHM area and its surroundings were previously muddy and sandy coastal areas. During reconnaissance on-site, determining geological formation is important for geologists and engineers as it is very useful in collecting various land information [12]. Refer to the geological map shown in Fig 1 this study area consists of unconsolidated deposits form of clay and silt (marine) [13]. In general, the presence of this type of material will exhibit a soft soil phenomenon due to its high-water content derived from the high-water table of lowland areas [14]. Moreover, the high rainfall intensity often occurs in tropical climate countries in Malaysia, contributing to the increase in the water table. Previous borehole results also found that this area consists of thick clay and silt. However, fine soil particles such as clay and silt can be associated with low hydraulic conductivity, affecting the effectiveness of groundwater recharge and the quality extracted from existing tube wells. Based on on-site observation and study by [14] verify that soft soil conditions related to wet clay and silt geomaterials dominate this study area. Thus, indicate the composition of the subsoil profile, which may consist of homogeneous soft soil geomaterials. Furthermore, the study area composed of clay and sit from the marine environment may influence the consistency of electrical resistivity value due to the possibility of an ancient seawater trap. A study by [15] has reported that ancient seawater that was trapped within sediment for a long time may influence groundwater characteristics. Due to ancient saltwater intrusion during the quaternary era and impacts of karts under the land surface had caused the water to contain a high concentration of calcium and chloride. In addition, a study by [16] verified that top and subsoil in the UTHM area is occupied by almost clay, in which the average rate of infiltration ranges from 0.004 mm/s to 0.076 mm/s.

2.2 Equipment

Three (3) spread lines (SL) were used in this study at each verified location in the UTHM surrounding area. Before the actual work can be conducted, several steps must be taken into account. Site accessibility, previous borehole data, and the proposed site area are several of the considerations that should be addressed before fieldwork. Fig. 2 shows the resistivity measurement equipment used in this study. The source, inducer, and record are the three main components of the equipment. The dry cell battery generates the data acquisition power source, while the steel electrode acts as a current inducer. The SAS 4000 thermometer is used to collect data on apparent resistivity. The equipment should be set up according to work procedures to reduce excessive reading errors after analysis. Furthermore, the study area should be free of any surface structures to avoid interruptions with the SL.

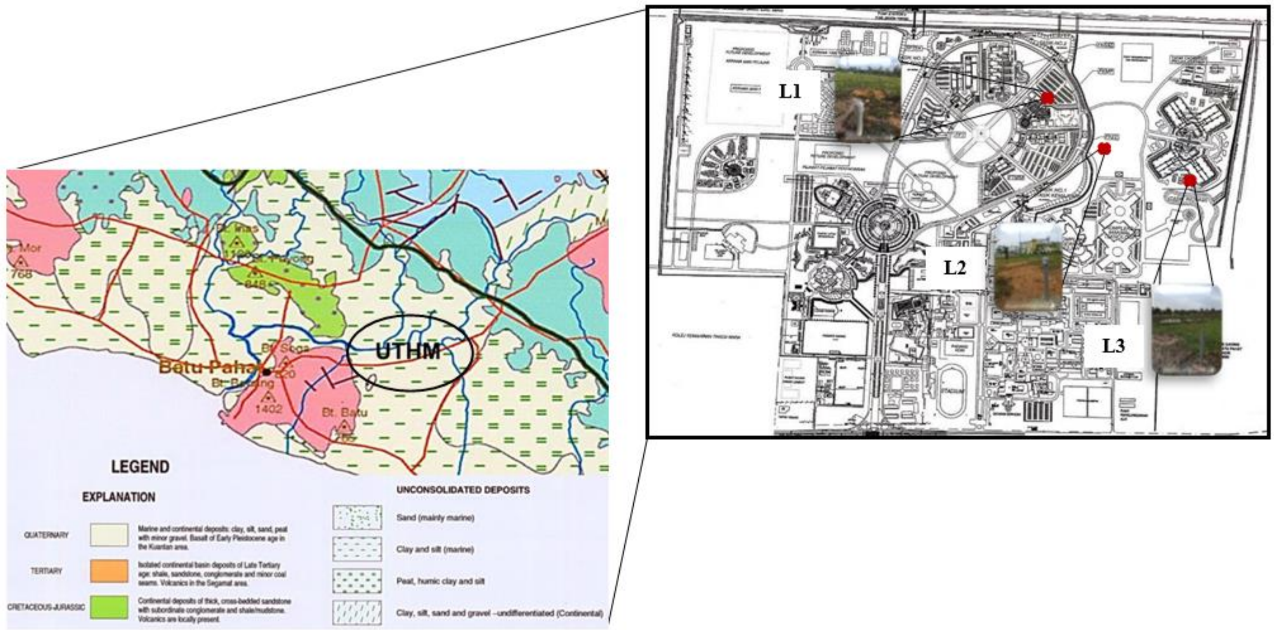

Fig. 1 - Geological map and the location of the study area [12]

Fig. 2 - Resistivity equipment set

During data acquisition, the Schlumberger array was chosen due to its ability to image deeper profiles and suitability for regions with homogeneous layers. Schlumberger current has slightly better horizontal coverage than the Wenner array. Furthermore, for the same distance, the median depth of this type of array investigation is 10% greater than that of the Wenner array [17]. A Schlumberger array with a distance of 2.5 m between electrodes was used, with a total layout length of 200 m (major line) and 150 m (minor line). This setup aimed to obtain a large number of total readings (data points), as a large number of data points will help reduce reading errors and increase data interpretation efficiency.

The resistivity line was set up in the field using a measuring tape to determine the proposed location area, which was required for electrode spacing. The spread line alignment was then established using three cables. The electrode was then tightly inserted into the ground for approximately two-thirds of its length to ensure good contact between the electrode and the ground. A jumper was then used to connect the electrode to the resistivity cable. A connector function is to connect long and short resistivity cables. The Terrameter SAS 4000 was placed in the center of the spread line, which was between the short and short lines after all of the equipment was correctly set up. Finally, the dry cell battery was connected to the Terrameter SAS 4000 to provide direct current during data acquisition. The current electrodes received and transferred the power supplied by the battery to the ground, while the other electrode received and transferred it to the instrument to complete the circuit. Potential capacity was measured with potential capacity electrodes (P1 and P2) injected between current electrodes (C1 and C2) [18]. Fig. 3 shows the ABEM Lund System standard field configuration. The coordinates for each electrode were recorded using GPS during data acquisition. In general, precautions are taken to reduce reading errors and prevent problems with the terrameter during data collection. The terrameter SAS 4000 was shielded from direct sunlight to prevent overheating. Excessive heat will reduce the equipment efficiency in obtaining the best data reading. Furthermore, dry ground conditions will affect resistivity detection because current flow cannot pass through the particle mass. As a result, water was poured at several points to ensure that the current could flow before the measurements were taken.

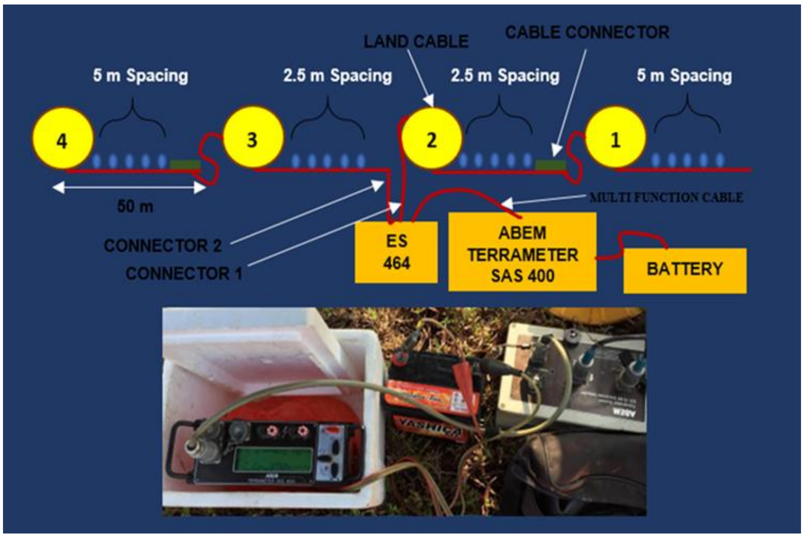

Fig. 3 - Standard field arrangement for ABEM Lund System in resistivity method

2.3 Data Interpretation

Terrameter SAS was used as a database to interpret the resistivity values of aquifer layers and select the compatible electrode configuration or array as the measuring method. Terrameter SAS 4000 was connected to an electrode selector via a cable terrameter in four (4) selected electrodes (a pair of current electrodes and a pair of potential electrodes to measure substance resistivity). The observed data are fictitious values that must be recalculated to obtain the final resistivity value. As a result, raw data is processed and interpreted with the RES2DINV software. The RES2DINV resistivity inversion software inverts apparent resistivity data from the field and automatically converts it to 2D imaging. To estimate the true resistivity of the subsurface, data were filtered to remove bad and inverted datum points [19]. RES2DINV is the least square inversion that uses the smoothing technique. The analysis employed a modified smoothness-constrained least-square method to generate subsurface imaging. In areas where the surface resistance is gradually changing, this inversion method produces better results. Furthermore, the inversion method minimizes the squared difference between measured and calculated resistivity values, resulting in a model of the earth's resistivity and gradual transition across zones [20]. The 2D imaging of a subsurface can be obtained using appropriate surveys and data interpretation techniques. The most prudent approach during data analysis is to select a model at the iteration where the Root Mean Square (RMS) error does not change significantly.

3. Result and Discussion

3.1 Location 1 (L1)

Referring to Fig. 4, the resistivity of the soil material beneath the spread line ranges between 1 and 80 m and mostly consists of clay. The top image shows the resistivity of the soil material while the bottom image shows the chargeability of soil materials. According to [17], the resistivity of clay and saturated silt ranged from 0 to 100 Ωm. Meanwhile, [2] found that fine soils such as clay and silt had low resistivity values, whereas coarse soils such as sand had higher resistivity values. Furthermore, the electrical resistivity to surface water (both natural and surface) varies between 1 and 100 Ωm [21]. Based on both ERV results, it was discovered that the subsurface profile was dominated by highly conductive material with ERV ranging from 1 to 80 Ωm. However, preliminary studies show that the surface area is mostly covered by clay material, and thus the data obtained can be verified. UTHM is also known as a marine clay-encircled area [22]. The left part of the region has a chargeability value less than 1 ms. [23] discovered that materials with similar chargeability values were alluvium composed of clay, silt, sand, or gravel. Furthermore, some parts of the region were discovered to have higher chargeability values than the surrounding materials at 86.25 m and 131.25 m from the first electrode. This region chargeability value ranges from 50 to 500 ms, may contain very fine sand or clay, such as shalestone [23]. The region with very low chargeability values was most prominently dispersed at 56.25 m from the first electrode at a depth of 20 m. This region has a chargeability value ranging from 0 to 0.9 ms, indicates the possibility of potential groundwater. On the other hand, the groundwater anomaly can be seen in the left center of Fig. 4.

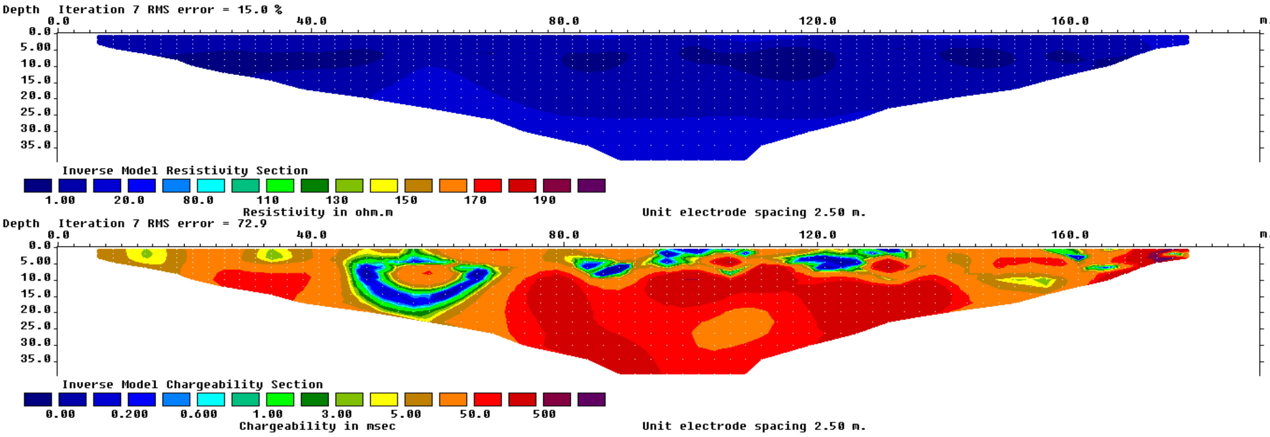

Fig. 4 - Spread line 1 imaging at Location 1

Meanwhile, in Fig. 5 the subsurface profile is composed of clay layers due to resistivity values ranging from 1 to 80 Ωm, which are similar to Fig. 4. Fine grain soils, such as clay and silt, have a higher mineral composition of kaolinite, montmorillonite, and vermiculite, allowing current soil propagation easier [24]. As a result, fine soils have lower resistivity values than coarse soils such as sand and gravel. The electrical resistance of soil is generally inversely proportional to its water content, whereas clay has a high concentration of soluble ions. Wet clay has the lowest ERV of any soil material, whereas coarse sand, gravel deposits, and hard bedrocks have the highest. Fig. 5 also shows that the subsurface profile is dominated by a low chargeability value, which could be interpreted as groundwater due to its IP value ranging from 0 to 1 ms. The electrical chargeability of groundwater is zero because of the very conductive material. Furthermore, according to [24], the chargeability of groundwater was 0 ms. Furthermore, minor spots in the region have higher chargeability values than surrounding materials 86.25 m from the first electrode. This region chargeability value ranges between 50 and 500 ms and may contain sandstone or consolidated clay, such as shale stone [23]. In general, the chargeability of common geomaterials can be influenced by clay content, sulphide mineralization, geomaterial discontinuity, or pore water salinity [25].

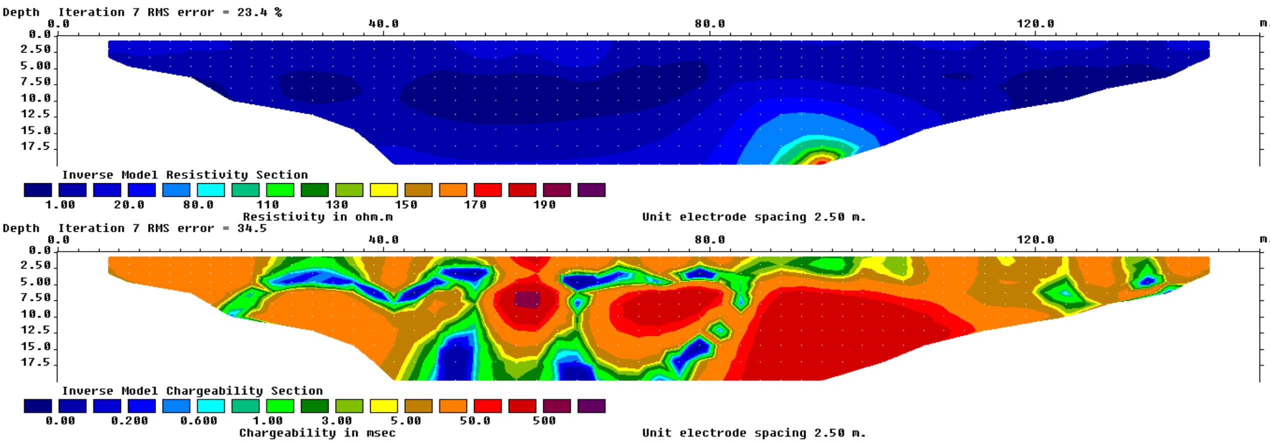

Fig. 5 - Spread line 2 imaging at Location 1

3.2 Location 2 (L2)

Subsurface profile mapping was generated based on tomography outcomes, as shown in Fig. 6. The subsurface layer beneath this line was dominant, with a resistivity value of less than 80 Ωm. However, the high resistivity value obtained (200 to 600 Ωm) at the right profile section located approximately 100 m to 150 m from the west indicated that this profile most likely obtained unconsolidated sediments such as alluvium [26]. Electrical methods can be difficult to apply in soft soil, especially during the interpretation stage due to contrast tomography. Furthermore, their highly conductive resistivity values allow electrical properties, particularly resistivity, to different geomaterial overlap values [25]. Meanwhile, the IP result revealed that low chargeability values of less than 1 ms dominated the right part of the spread line thus indicates the presence of groundwater. In addition, a very low chargeability value was distributed throughout the layer. The potential location of shallow groundwater is 120 m to 160 m from the first electrode, at 20 m below the ground surface. As previously stated, interpreting groundwater potential in highly conductive geomaterials such as clay and silty soil is difficult due to overlapping clay, silty, and groundwater values. Thus, IP reduces the problem by distinguishing geomaterial types based on the small value of their chargeability, as described in [23]. The interpretation from IP imaging assisted in indicating potential groundwater because the chargeability value obtained from the electrical resistivity method can distinguish between groundwater and clay.

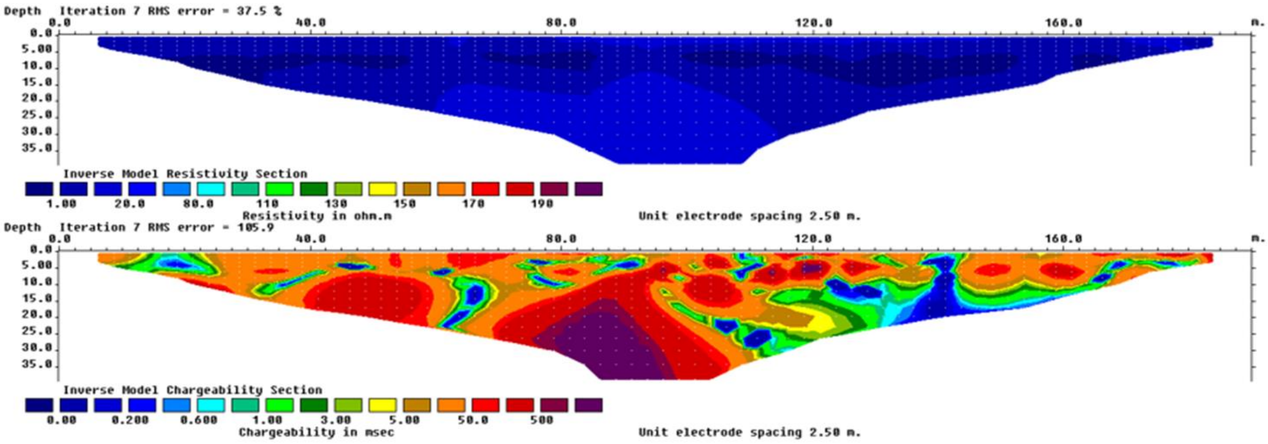

Fig. 6 - Spread line 1 imaging at Location 2

Fig. 7 shows the different ERV obtained for this profiling when compared to spread lines 1. The two-resistivity distribution ranged from 0.1 to 80 Ωm (low ERV) to 200 to 600 Ωm (high ERV). By varying depths to 30 m below the surface, the low resistivity value is indicated by the blue color observed at the centre of the profiling. However, high ERV up to 600 Ωm were verified on the left and right sides of the profile, until 20 m from the surface layer. According to [17], ERV between 20 and 800 Ωm may be considered alluvium. The electrode was also difficult to plug in due to the hard surface layer of soil, as observed during data acquisition. Meanwhile, low chargeability values were distributed only on the nearest surface layer for IP imaging. Unlike the IP profiles of spread lines 1, this layer was predominantly covered with high chargeability values. Because it may contain sandstone or highly consolidated clay, such as shalestone since the chargeability value of this region ranged from 50 to 500 ms [23]. To validate the data obtained, a correlation between ERI and the boring technique was required.

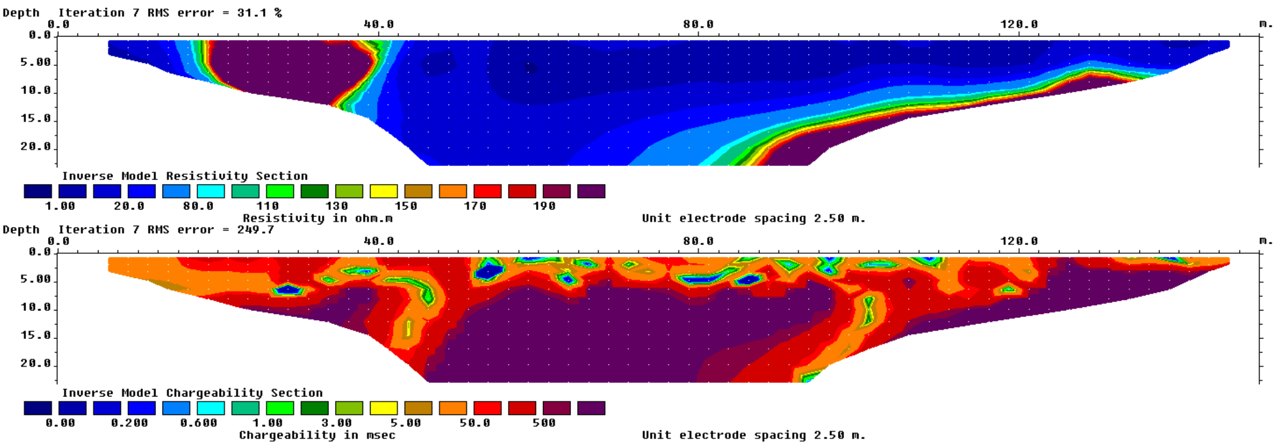

Fig. 7 - Spread line 2 imaging at Location 2

3.3 Location 3 (L3)

Major spread lines of 200 m and minor spread lines of 150 m were set up in this location. Fig. 8 imaging shows that the resistivity value of the soil beneath the spread line ranges from 0.1 to 50 m. This layer mainly consisted of clay.

When compared to the results of L1 and L2, the layers showed different variation. In general, the electrical resistivity of soil is inversely proportional to its water content. Meanwhile, clayey soil has a high concentration of dissolved ions, while wet clayey soil has the lowest resistivity of all soil materials. However, the chargeability image contains more data variety than the resistivity image. Based on the IP imaging, it has been determined that a very low chargeability region could be observed. The layer is mostly covered with groundwater and is located approximately 5 to 20 m underground with a chargeability value of 0 to 1 ms. The area with a high expectation of potential shallow groundwater was 65 m to 150 m from the first electrode. Parts of the region have higher chargeability, such as at 78.75 to 120 m from the first electrode, which increases the chargeability value from 20 to 500 ms, forming an oval-shaped region about 8 m below the ground surface. [27] classified minerals with comparable chargeability as sandstones or siltstones. Furthermore, based on on-site observations during data acquisition, this spread line was located near buildings where the layer beneath is close to the pipeline.

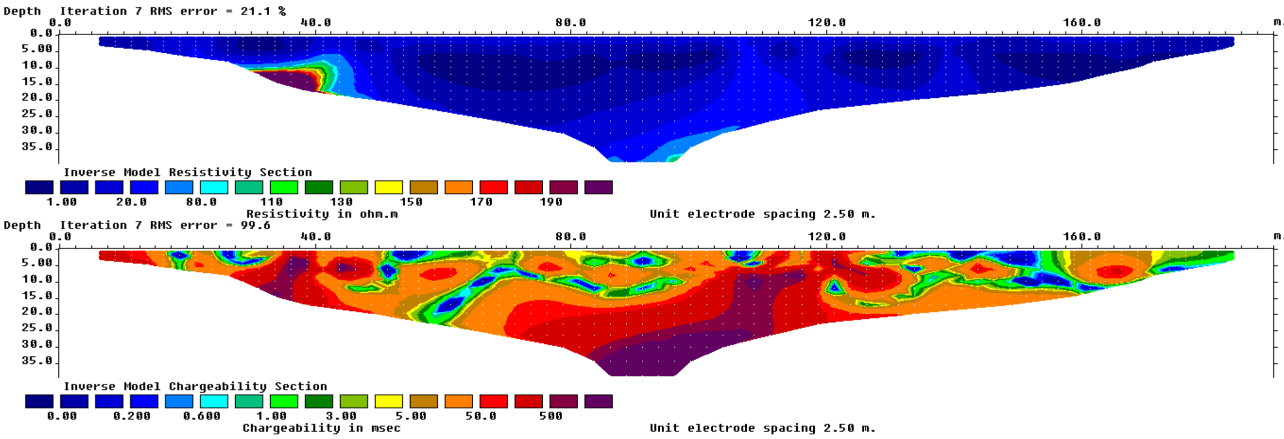

Fig. 8 - Spread line 1 imaging at Location 3

Meanwhile, on the electrical results shown in Fig. 9, it was discovered that the subsurface profile was dominated by highly conductive material with a resistance value ranging from 1 to 80 Ωm and a chargeability value of less than 1 ms which this layer was mostly form of clay. The geological map showed that the land was mostly covered in clay, which matched the resistivity result. However, chargeability imaging shows that the layer can be classified based on the chargeability of the soil material. Most regions have a chargeability value ranging from 0.1 ms to 4 ms. [23] suggested that the material with such a chargeability value might be alluvium. Furthermore, regions with high chargeability values were scattered throughout the IP image but were present most notably at the left and right side of the IP image. The chargeability value of that specific region, which ranges from 50 ms to 500 ms, may contain sandstone or highly consolidated clay. Furthermore, a region with a very low chargeability value was discovered at 123.75 m to 140 m, a depth of 3 m to 15 m, and a chargeability value of 0 to 0.4 ms. Thus, indicates that groundwater may exist in the zones. Table 1 summarizes the findings from the three locations in this research area.

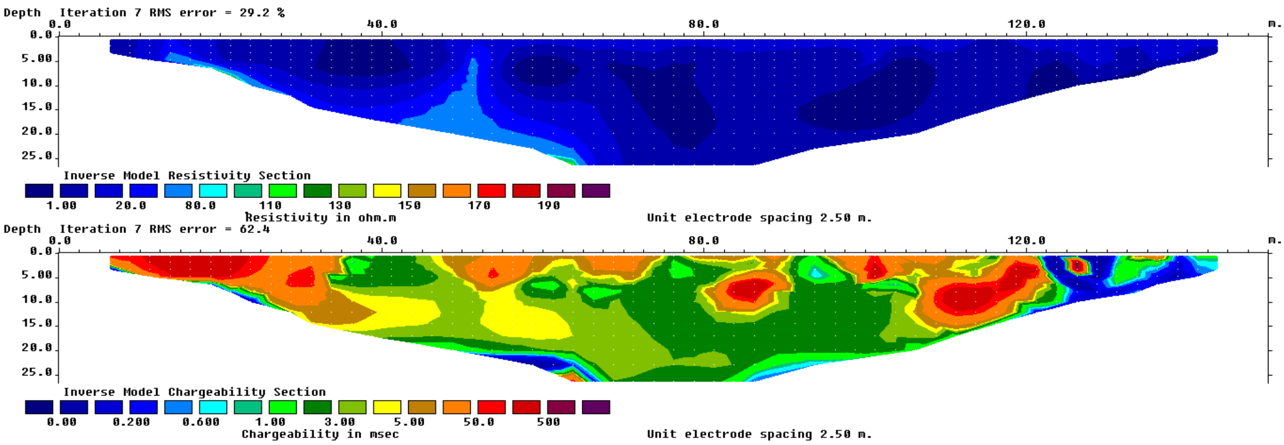

Fig. 9 - Spread line 2 imaging at Location 3

Table 1 - Resistivity and chargeability value for the three locations

Location / Parameter	Location 1 (L1)	Location 2 (L2)	Location 3 (L3)
Resistivity value	1 to 7 Ωm	1 to 8 Ωm	1 to 20 Ωm
Chargeability value	0 to 1 ms	0 to 1 ms	0 to 1 ms

4. Conclusion

ERI and IP successfully replicated the subsurface profile in the study area. By analysing the electrical resistivity and chargeability data, the properties of the resistivity and chargeability distribution of the subsurface profile in the study area were determined, and the results obtained generally show very good agreement with previous references. According to the results of the analysis using the RES2DINV software, the three study locations have a good potential of groundwater sources as referred to the electrical images with low resistivity values that verify between 1 and 20 Ωm, which is similar to a study by [23] in the same study area. Some constraints, such as site accessibility and geological conditions in the study area, may affect the depth of the groundwater image and the effectiveness of rechargeability. Furthermore, the geological conditions of this area (quaternary deposits geomaterials) may impact groundwater performance in terms of recharge capacity. The groundwater potential is essentially located at an average of 10 to 30 m from the ground surface. Thus, ERI is capable in indicate shallow aquifers for water resources [28].

Acknowledgement

Communication of this research is made possible through monetary assistance by Universiti Tun Hussein Onn Malaysia and the Pejabat Pendaftar with Vot H530 Geran Penyelidikan Pascasiswazah (GPPS).

References

[1] Dor N., Syafalni S., Abustan I., Rahman M. T. A., Nazri M. A. A., Mostafa R. & Mejus L. (2011). Verification of surface-groundwater connectivity in an irrigation canal using geophysical, water balance and stable isotope approaches. Springer : Water Resources Management, 25(11), 2837–2853.

[2] Abidin M. H. Z., Saad D. R., Ahmad F., Wijeyesekera D. C. & Baharuddin E. M. F. T. (2011). Application of geophysical methods in civil engineering. Proceeding of Malaysian Technical Universities International Conference on Engineering and Technology (MUiCET 2011), Johor, Malaysia.

[3] Asry Z., Samsudin A. R., Yaacob W. Z. & Yaakub J. (2012). Groundwater exploration using 2-D geoelectrical resistivity imaging technique at Sungai. Udang, Melaka. Journal of Earth Science and Engineering, 2(October), 624–630.

[4] Azhar A. T. S., Hazreek Z. A. M., Aziman M., Haimi D. S. & Hafiz Z. M. (2016). Acidic barren slope profiling using electrical resistivity imaging (ERI) at Ayer Hitam area Johor, Malaysia. Journal of Physics: Conference Series, 710(012008), 1–10.

[5] Loke M. H., Acworth I. & Dahlin T. (2003). A comparison of smooth and blocky inversion methods in 2D electrical imaging surveys, Exploration Geophysics, 34(3), 182-187.

[6] Zainal Abidin M. H., Tajul Baharuddin M. F. & Kamarudin A. F. (2010). Application of Geoelectrical Method in Subsurface Profile Forensic Study. Proceedings of Malaysian Technical Universities Conference on Engineering and Technology (MUCET), Melaka, Malaysia.

[7] Metwaly M., Elawadi E., Moustafal S. S., Fouzan F. Al, Mogren S. & Arifi N. Al. (2012). Groundwater exploration using geoelectrical resistivity technique at Al-Quwy'yia area Central Saudi Arabia. International Journal of the Physical Sciences, 7(2), 317–326.

[8] Diat K. A. N. A., Awawi M. N. M. N. & Bdullah K. A. (2013). Application of multi-criteria decision analysis to geoelectric and geologic parameters for spatial prediction of groundwater resources potential and aquifer evaluation. Pure and Applied Geophysics, 170, 453–471.

[9] Musa S., Azazi N., Tjahjanto D. & Sai L. (2009). The potential of recharge well system in flat area with low infiltration rate. Proceeding of International Conference on Water Resources (ICWR 2009), Kedah, Malaysia.

[10] Musa S., Ahmad Nazri M. A. & Abdul Kadir A. (2016). Simplified method for groundwater treatment using dilution and ceramic filter. IOP Conference Series: Materials Science and Engineering, 136, 1–10.

[11] Adnan M. S., Mohamad N., Adib M., Razi M., Musa S. & Rosly N. (2016). Investigation of groundwater flow in clay aquifer in Parit Raja Catchment. ARPN Journal of Engineering and Applied Sciences, 11(16), 9848–9854.

[12] Noor M. A. M., Madun A., Kamarudin A. F. & Daud M. E. (2015). A study of geological formation on different sites in Batu Pahat , Malaysia based on HVSR method using microtremor measurement. IOP Conference Series:

Materials Science and Engineering, 12, 012038,
[13] Aziman M., Hazreek Z. A. M., Azhar A. T. S., Fahmy K. A., Faizal T. B. M., Sabariah M. & Ismail M. A. M. (2018). Electrical resistivity technique for groundwater exploration in quaternary deposit. Journal of Physics: Conference Series, 995(1), 1–8.
[14] Hazreek M., Abidin Z., Madun A., Azhar S. & Tajudin A. (2017). Evaluation of unknown tube well depth using electrical resistivity method. Materials science, Engineering and Chemistry (MATEC) Web of Conferences, 7002, 13.
[15] Samsudin A. R., Haryono A., Hamzah U. & Rafek A. G. (2008). Salinity mapping of coastal groundwater aquifers using hydrogeochemical and geophysical methods : A case study from North Kelantan, Malaysia. Environment Geology, 55(10), 1737–1743.
[16] Adnan M. S., Aliff M., Anuar M. & Nda M. (2017). Investigation of infiltration rate on soft clay that affecting the ponding time. Materials science, Engineering and Chemistry (MATEC) Web of Conferences, 103, 04021.
[17] Loke M. H. (1999). A practical guide to 2-D and 3-D surveys. Electrical imaging surveys for environmental and engineering studies. E-Publishing, 1-67.
[18] Martorana R., Capizzi P., Alessandro A. D. & Luzio D. (2016). Comparison of different sets of array configurations for multichannel 2D ERT acquisition. Journal of Applied Geophysics, 3163, 1–38.
[19] Jayeoba A. & Oladunjoye M. A. (2015). 2-D electrical resistivity tomography for groundwater exploration in hard rock terrain. International Journal of Science and Technology, 4(4), 156–163.
[20] Seaton W. J. & Burbey T. J. (2002). Evaluation of two-dimensional resistivity methods in a fractured crystalline-rock terrane. Journal of Applied Geophysics, 51(1), 21–41.
[21] Telford W. M. Geldart L. P, Sheriff R. E. & Kays D. A. (1976). Applied geophysics. Press New York.
[22] Keller G. V. & Frischknencht F. C. (1996). Electrical methods in geophysical prospecting. Pergamon Press.
[23] Riwayat A. I., Nazri M. A. A. & Abidin M. H. Z. (2018). Detection of potential shallow aquifer by using electrical resistivity imaging (ERI) at UTHM Campus, Johor Malaysia. Journal of Physics: Conference Series, (1)995, 1-8.
[24] Telford W. M. & Sheriff R. F. (1990). Applied geophysics. Press New York.
[25] Abidin M. H. Z., Ab. Ghani A. R., Ahmad Tajudin S. A., Abu Talib M. K. & Riwayat A. I. (2017). Preliminary Groundwater assessment method at quaternary deposits area using electrical. IOP Conference Series: Materials Science and Engineering, 226, 12042.
[26] Wilkinson P. B., Loke M. H., Meldrum P. I., Chambers J. E., Kuras O., Gunn D. A. & Ogilvy R. D. (2012). Practical Aspects of applied optimized survey design for electrical resistivity tomography. Springer, 428–440.
[27] Montgomery C. W. (2006). Environmental geology. McGraw Hill International.
[28] Riwayat A. I., Nazri M. A. A. & Abidin M. H. Z. (2018). Application of Electrical Resistivity Method (ERM) in Groundwater Exploration. Journal of Physics: Conference Series, (1)995,1-10.